The gut microbiota confers the glucose-and lipid-lowering effect of Laurolitsine in db/db mice

Rui-qi Wang
Hainan Medical University
Fang Zhang
Chinese Academy of Medical Sciences & Peking Union Medical College
Ya-nan Yang
Chinese Academy of Medical Sciences & Peking Union Medical College
Yin-feng Tan
Hainan Medical University
Yong Zhang
Hainan Medical University
Lin Dong
Hainan Medical University
Ning Ma
Hainan Women and Children's Medical Center
Wei-ying Lu
Hainan Women and Children's Medical Center
Chong-ming Wu
Chinese Academy of Medical Sciences & Peking Union Medical College
Xiao-po Zhang (z_xp1412@163.com)
Hainan Medical University

Research Article

Keywords: Laurolitsine, diabetes, anti-hyperglycemia, anti-hyperlipidemic, Intestinal microflora

Posted Date: November 3rd, 2021

DOI: https://doi.org/10.21203/rs.3.rs-1003097/v1

Abstract

Background

Modulations on gut microbiota by traditional Chinese medicines (TCMs) and their active components are emerging as potential therapeutic agents on diabetes. *Litsea glutinosa* is a TCM used in clinic to treat diabetes with alkaloids as the active constituents, and the Laurolitsine is the richest one.

Purpose

Based on that, this study was designed to identify the potential capability of Laurolitsine on alleviating Type 2 diabetes and the changes of the composition of intestinal flora related to this disease.

Methods

In present study, Laurolitsine was administered to diabetic mice (db/db) by daily oral gavage at doses of 50, 100 and 200 mg/kg/day for 4 weeks. The body weight, fasting blood glucose, oral glucose tolerance test (OGTT) and insulin tolerance test (ITT), lipid metabolism of serum and liver and liver function were measured to assess the anti-hyperglycemic and anti-hyperlipidemic effects of Laurolitsine. The liver pathological changes were observed by HE staining. Meanwhile, the effects of Laurolitsine on the changes of the composition of gut microbiota in mice were investigated via metagenomic analysis.

Results

Experimental results show that different doses of Laurolitsine have varying degrees of hypoglycemic and hypolipidemic effects. Among them, the treatment effect of 200mg·Kg^{-1} is the most obvious. In addition, Laurolitsine changes the structure of intestinal microflora significantly at various taxonomical levels in the diabetic db/db mice.

Conclusions

These results demonstrate that Laurolitsine may regulate glucose and lipid metabolism and improve diabetes through modulating intestinal microflora of *Parabacteroides* and *Mucispirillum*, which may be acknowledged as the iconic bacteria of diabetes.

Introduction

Type 2 diabetes is a chronic disease caused by genetic and environmental factors (Bysani, Agren et al. 2019), and insulin resistance is the main pathophysiological mechanism. The International Diabetes

Federation showed that the number of people aged 20-79 years with diabetes mellitus (DM) worldwide was estimated to be 463 million in 2019. Almost 90% of these people will have type 2 diabetes mellitus (T2DM), and this number may increase to 700 million by 2045 (Caron, Ahmed et al. 2020). Oral anti-diabetic agents include sulfonylureas, biguanides, thiazolidinediones, alpha-glucosidase inhibitors, meglitinides and etc (Wu, Huang et al. 2019). However, these treatments have appreciated side effects with unsatisfactory clinical benefits. Therefore, the discovery and development of safer and more effective hypoglycemic drugs is of great significance to overcome this global disease. Intestinal microflora is a microbial community in the human intestinal tract, which participates in digestion, absorption, metabolism, nutrition, and immunity to infection of in the human body (Ke, Walker et al. 2019). Researches demonstrated that the changes in the structure and function of intestinal microflora are closely related to diabetic phenotypes such as hyperglycemia and insulin resistance (Chen, Li et al. 2017). Intestinal microflora and their related metabolites play an important role in the pathophysiological mechanisms of type 2 diabetes such as blood glucose metabolism, insulin resistance and chronic inflammation (Molinaro, Koh et al. 2020, Toda, Soeda et al. 2020). Therefore, regulating the structure of intestinal flora in patients with type 2 diabetes is expected to become a new way to pretreat type 2 diabetes.

Most TCMs play their role through oral administration, and the drugs entering the digestive tract inevitably modulate intestinal microenvironment and the structure of intestinal microflora (Gao, Yang et al. 2018, Liu, Zhang et al. 2018, Zhang, Yue et al. 2019). At the same time, TCMs was metabolized and transformed by reductive and hydrolysis reactions of intestinal microorganisms, and then be absorbed by the human body to achieve a therapeutic effect. Therefore, there is a close relationship between intestinal flora and the efficacy of traditional Chinese medicine, and intestinal flora is likely to be the target of its efficacy.

Litsea glutinosa is a TCM belonging to *Lauraceae* and is distributed in tropical and subtropical region worldwide. In China, this plant is mainly growed in Hainan Province. Our group has been engaged in structure and function of *Litsea glutinosa* for a long time. Previous research showed that the extract of *L. glutinos*a could significantly reduce the blood glucose in ob/ob mice (Zhang, et al. 2018). Moreover, Lignans, alkaloids were the characteristic components of *L. glutinosa* (Ji et al.; Jin et al., 2018), which of the Laurolitsine (LL) was found at a high concentration in the gastrointestinal tract by our group recently (Tan et al., 2021). Thus, this study aimed to investigate whether LL treatment prevents the development of Type 2 diabetes and modulates gut microbiota dysbiosis in diabetic mice. More importantly, we aimed to identify potential correlations between LL treatment and changes in the gut microbiota, providing solid insight into gut microbiota-related mechanisms underlying the anti-diabetic effects of LL.

Materials And Methods

Plant material

The stem barks of *L. glutinosa* were collected in August 2019 in Tongguling, Wenchang City, Hainan Province, and identified by Prof. Niankai Zeng from the Department of Pharmacy at Hainan Medical University. A voucher specimen (No. LG201908) was deposited at the herbarium of School of Pharmacy, Hainan Medical University.The study protocol complied with relevant institutional, national, and international guidelines and legislation.

Preparation of LL

The dried stem barks (100.0 Kg) of *L. glutinosa* were cut into small pieces. Ethanol was then used to extract the plant under reflux for three times, each time for 2 hours. The extract was concentrated under reduced pressure till there is no ethanol to give the water solvent of the extract. Appropriate water was added and then extracted by petroleum ether to remove the lipid solvable constituents. Then the mother liquid was further extracted by ethyl acetate to give the total alkaloids. The total alkaloid was isolated by applying a silica gel chromatography using a mixture of dichloromethane: acetone = 4:1 to give six fractions (Fra1-Fra6). Fra4 was further purified by using Sephadex LH-20 using methanol as the eluent to give three subfractions (Subfra1-Subfra3). Subfra2 was purified by preparative equipped with a SB-phenyl column using a mixture of methanol: water = 65:35 as the eluent to give the LL (8.0 g).

Structural identification of LL

The structural identification of LL was conducted by interpreting its NMR and MS data. NMR experiments were performed on ECZ400S 400 MHz spectrometers operating at 400 MHz for ^{1}H and 100 MHz for ^{13}C, respectively (TMS as an internal standard). Chemical shifts were expressed in δ (ppm), and coupling constants in Hz. MS experiment was conducted on an HPLC-MS/MS system. The HPLC system was equipped a SIL-20AC^{XR} autosampler, two LC-20AD^{XR} pumps, an online degasser, and a CTO-20A column oven, and they were all purchased from Shimadzu (Kyoto, Japan). The chromatographic column was Synergi™ Fusion-RP 80 Å C_{18} (4 μm, 2.10 mm i.d × 50 mm, Phenomenex, Torrance, CA, USA), the temperature was maintained at 40 °C during analysis. The aqueous solution containing 0.5% formic acid (A) and acetonitrile with 0.5 % formic acid (B) made up the mobile phase. The gradient elution was 5% B at 0-3 min, 35 % B at 3-3.5 min, 95% B at 3.5-5min, 5% 5-6.5 min. The flow rate was set at 0.3 mL/min and the injection volume was 5μL. An AB Sciex Triple Quad^{TM} 5500 system was operated in the electrospray positive ionization mode (ESI^{+}). The MS analysis detection was optimized when the collision energy was at 18 volt. The optimized declustering potential was 80 volt, temperature, 55 °C; curtin gas, 55psi; nebulizer gas, 60psi; ion spray voltage, 5500, scan time, 40ms.

The determination of purification of LL

The purity of LL was determined to be 98.73% by our group using HPLC method. The column was C_{18} (4.6 × 250 mm, 5.0 μM), the detection wavelength was set at 282 nm. The flow rate was 1.0 mL/min. The column temperature was set at 30 °C, the mobile phase was phase A (acetonitrile), phase B was

triethylamine-phosphoric acid in water (pH = 7.0), and the gradient elution was set at A 15-25% for 20 min.

Animals

Animal experiments were carried out according to the National Institutes of Health guides for the care and use of laboratory animals and were approved by the Medical Ethics Committee of Hainan Medical University (No. SYXK-2017-0013). The study is reported in accordance with ARRIVE guidelines. Ten 8-week old male C57BL/KsJ mice with a body weight of 20-25g and sixty db/db mice were obtained from GemPharmatech. Co,. LTD (Nanjing China).

Experimental designs

After 1 week of acclimatization, the db/db mice were randomly divided into 5 groups, including model group (n = 10), LL 50 $mg \cdot Kg^{-1}$ group (n = 10), LL 100 $mg \cdot Kg^{-1}$ group (n = 10), LL 200 $mg \cdot Kg^{-1}$ group (n = 10), and metformin 200 $mg \cdot Kg^{-1}$ (n = 10). The normal group (C57BL/KsJ group (n = 10)) was given a standard rodent chow diet and db/db mice were fed with high-fat diet (HFD) for 4 weeks. Both LL and metformin were dissolved in normal saline and were given by intragastric administration at 14:00 every day for 4 weeks. The normal and negative model groups were gavaged with equal volume of normal saline. Body weight was recorded every five day. Water uptake and food intake was recorded every week. After fasting for 12 h every week, blood samples were taken from the tail vein to detect fasting blood glucose.

OGTT and ITT measurements

Oral Glucose Tolerance Test (OGTT) and insulin tolerance test (ITT) was performed one day before the terminal sacrifice. Mice were fasted for 12 h (OGTT) or 6 h (ITT). Next, a solution of 25% glucose (2 $g \cdot Kg^{-1}$ body weight) was administered into the peritoneal cavity for the OGTT or a solution of insulin (0.5 $U \cdot Kg^{-1}$ body weight) for the ITT. Blood samples were collected from the tail vein at 0, 30, 60 and 90 min for the determination of blood glucose levels and the area under curve (AUC) of OGTT and ITT was calculated for respective groups and used for statistical analysis.

Measurements of levels of lipid, AST and ALT in serum and liver

After 4 weeks of LL treatment, all mice were fasted for 8 h before sacrifice. The whole blood was obtained from the orbital vascular plexus and blood samples were collected for estimation of serum levels of total triglyceride (TG), total cholesterol (TC), low-density lipoprotein cholesterol (LDL-c), and high-density lipoprotein cholesterol (HDL-c) by respective kits (Nanjing Jiancheng Bioengineering Institute). Liver tissues were taken for the subsequent histological analysis. Otherwise, liver levels of TG, TC, LDL-c, HDL-c, aspartate aminotransferase (AST), and alanine aminotransferase (AST) were measured.

H&E Staining

The fresh liver tissues were fixed in 4% paraformaldehyde. Then, the samples were gradually dehydrated and embedded in paraffin. After that, the samples were cut into 3 μm sections and stained with hematoxylin and eosin for further light microscopy observation. Scores were evaluated by a pathologist based on the lung tissue integrity, alveolar integrity, and mononuclear infiltration (0 = none; 1 = mild; 2 = moderate; 3 = severe).

Metagenomic analysis

Fresh stool were collected from each mouse, snap-frozen in liquid nitrogen, and stored at − 80 °C for subsequent metabolomics analysis. Fecal DNA extraction using a FastDNA® Spin Kit for Stool, 16S rRNA V4–V5 regions amplification by barcoded composition primers. The PCR reaction was performed as follows: 95 °C for 5 min, followed by 30 cycles of 95 °C for 30 s, 55 °C for 30 s and 72 °C for 30 s, with a final extension at 72 °C for 5 min. The amplicons were pooled and purified using a QiaQuick PCR purification kit (Qiagen, Valencia, USA) and DNA pyrosequencing was performed by Majorbio BioTech Co., Ltd. (Shanghai, China) according to the methods mentioned in the literature(Li, Yang et al. 2018).

Data analysis

For phylotypes analysis, the alpha diversity of the microbiome was calculated based on the OTU level by mothur (version 1.30.1). Principal component analysis (PCA) and principal coordinate analysis (PCoA) were performed using R and visualized by the R package, whose significant differences were evaluated by Adonis analysis. All data presented in this paper are shown as mean standard error of the mean (SEM). For pharmacological results, comparisons between groups were assessed by one-way analysis of variance (ANOVA) with Dunnett's test as a post hoc test. A P value of <0.05 was considered statistically significant.

Results

Structural identification of LL

The alkaloid was brown powder, showed positive reaction with dragendorff's reagent. The MS spectrum showed an ion peak at *m/z* 314.2 $[M+H]^+$ (Figure 1A). The ^{1}H-NMR (400 MHz, CD_3OD) spectrum displayed signals attributable to two phenyl rings at δ_H 7.95 (1H, brs, H-11), 6.68 (1H, s, H-8), 6.54 (1H, s, H-3), and two methoxyls at δ_H 3.83 (3H, s, 10-OCH_3), 3.55 (3H, s, 1-OCH_3), three methanes at δ_H 3.30 (1H, m, H-5a), 2.96 (1H, m, H-5b), 2.70 (1H, m, H-7a), 2.58 (1H, m, H-7b), 2.96 (1H, m, H-4a), 2.67 (1H, m, H-4b) and one methine at δ 3.73 (1H, m, H-6a) (Figure S1A). These data indicated that this compound was an aporphine alkaloid. The above elucidation was confirmed by its ^{13}C-NMR (100 MHz, CD_3OD) spectral data at δ_C: 151.0 (C-2), 147.8 (C-10), 147.2 (C-9), 144.5 (C-1), 130.3 (C-7a), 129.8 (C-3a), 127.7 (C-3b), 126.0 (C-11b), 124.7 (C-11a), 115.8 (C-8), 115.5 (C-11), 112.8 (C-3), 60.3 (10-OCH_3), 56.5 (1-OCH_3), 54.8 (C-6a), 43.5 (C-5), 36.4 (C-7), 28.5 (C-4) . After carefully comparing its 1D-NMR and 2D NMR data with literature, the compound was determined to be Laurolitsine, and its molecular structure was depicted in

Figure 1A. The purity of LL was determined to be over 98% by our research group using HPLC method (Figure 1 B). With this extractive craft, we got 8.0g LL from the 100 kilogram dried stem barks of *L. glutinosa*.

Modulation of body weight, food intake and water uptake by LL

In order to observe the effects of LL on the body weight, food and water intake of db/db mice, we chose 50, 100 and 200 $mg \cdot Kg^{-1}$ as the low, medium and high dose of LL in mice. The body weight of mice was measured every five days, it was found that the body weight of mice in C57BL/KsJ group was almost stable, but the body weight of mice in the model and administration group increased gradually over time.

Besides, the body weight of the model mice was significantly higher than that of the C57BL/KsJ group, but there was no significant difference between the model group and LL group (Figure 2A). In addition, food intake and drinking water tended to be stable in the control group. However, food intake decreased slightly and drinking water increased slightly in the model and administration group (Figure 2B and 2C). Therefore, the treatment of LL had a little effect on the body weight, diet and drinking water of mice.

Effects of LL treatment on blood glucose

Then, we evaluated the effect of LL on blood glucose in db/db model mice. Results showed that the fasting blood glucose of mice in the model group was significantly higher than that of the control group ($P < 0.001$). Compared with the model group, LL could reduce the level of fasting blood glucose in a dose-dependent manner ($P < 0.001$). The hypoglycemic effect of 200 $mg \cdot Kg^{-1}$ was similar to that of metformin group (Figure 3A). Moreover, oral glucose tolerance test showed that the blood glucose of the model group still remained a high level after glucose administration, indicating that the glucose tolerance and the ability to consume glucose were decreased, while LL could significantly reduce the level of blood glucose after 30min ($P < 0.001$), and the effect of 200mg/kg was similar to that of metformin. In addition, insulin tolerance test showed that LL treatment can also rapidly reduce the level of blood glucose and improve insulin resistance after insulin injection (Figure 3B and 3C). These data demonstrate that LL has the potential capability to restore the disorder of glucose metabolism in db/db diabetic mice.

The effects of LL on lipid metabolism of serum and liver

At the same time, we detected the effect of LL on lipid metabolism in serum and liver of mice in each group. The results showed that 200$mg \cdot Kg^{-1}$ LL treatment showed a trend to normalize hyperlipidemia, especially on decreasing the levels of TC ($P < 0.05$) and TG ($P < 0.01$) in serum and liver, LDL-c ($P < 0.01$) and HDL-c ($P < 0.01$) in serum, but failed to reach statistical significance on restoring the level of LDL-c and HDL-c in liver (Figure 4A-H). Metformin treatment also had no significant effect on liver HDL-c (Figure 4H). Taken together, these results verified that LL treatment effectively ameliorated hyperlipidemia in db/db mice.

The effects of LL on liver function

Besides, we also examined the effect of LL on liver function. Histopathological profile of mice in C57BL/KsJ group showed normal hepatocytes with well cytoplasm, prominent nucleus, nucleolus and central vein with no sign of inflammation or necrosis in these mice. In model group, liver sections showed hepatocyte nuclear pyknosis, hepatic cord degeneration, inflammatory infiltration, and marked necrosis. Treatment with LL at 50, 100 and 200 $mg{\cdot}Kg^{-1}$ dose showed reduction of necrosed area and inflammatory infiltrates (Figure 5A and 5D). These results indicated that LL could ameliorate the severity of liver damage in db/db mice. Serum aminotransferase such as alanine aminotransferase (ALT) and aspartate aminotransferase (AST) are commonly used as an indicator for liver disease (Yang, Chen et al. 2020). In the present study a significant elevation of serum ALT and AST activities ($P < 0.05$) were observed in model mice. However, LL at 50, 100 and 200 $mg{\cdot}Kg^{-1}$ dose prevented these elevations in a dose-dependent manner, in which mice treated with 200 $mg{\cdot}Kg^{-1}$ LL group showed a significant reduction in serum ALT and AST (Figure 5B and 5C). In addition, it is well-established that the serum lactate level indicates glycolytic status in mice. The liver has a strong ability to remove blood lactic acid, so the level of blood lactic acid will increase in varying degrees when liver function is impaired. Mice in model group showed much higher levels of serum lactate than mice in C57BL/KsJ group (Figure 5E), indicating a lower glycolytic rate in model mice, LL at 100 and 200$mg{\cdot}Kg^{-1}$ dose can reduce serum levels of lactate but no significant difference. In summary, these results show that LL can somewhat recover liver injury in db/db mice.

The effects of LL on diversity of gut microbiota

The gut microbiotas play essential roles in the incidence and development of many diseases such as obesity, hyperlipidemia and T2DM. To check the influence of LL on the gut microbes, we firstly assessed the diversity of the gut microbiota by 16S rDNA-based metagenomic analysis. The results showed that the Shannon, Simpson, inverse Simpson, Richness and Evenness in the model group were decreased significantly, but there was little effect on these indexes of α-diversity after LL treatment (Figure 6A-E). In addition, we observed the changes of β-diversity of intestinal flora by PCA (Figure 6F) and PCoA (Figure 6G) analysis. Compared with normal group, the intestinal flora of mice in the model group was almost isolated along the PC1 direction in PCA analysis (Figure 6F) and along the PCo1/2 directions in PCoA analysis (Fig. 6G). In summary, LL had slight effects on the diversity of intestinal flora.

The effects of LL on composition of gut microbiota

Taxonomic analysis also displayed a marked impact of LL on gut microbes (Figure 7). At the phylum level, compared with the normal group, *Deferribacteres* and *Firmicutes* increased and *Bacteroidetes* decreased in the model group, which could be reversed by the LL group. Moreover, LL treatment can also decrease Viruses_noname and increase Fusobacteria in mice feces (Figure 7A). The genus-level analysis showed that the genera in the model group with a significant decrease in abundance were *Parabacteroides, Alphapapillomavirus and Clostridium,* while the genera with a significant increase in abundance were *Anaerotruncus*, *Escherichia* and *Mucispirillum*, t*he administration* of LL *reversed* these changes markedly (Figure 7B). At the species levels, oral administration

of LL enriched *Parabacteroides_unclassified*, yet decreased *Anaerotruncus_sp_G3_2012, Mucispirillum_schaedleri* and *Clostridium sp ASF502* with the same trend. Then we use linear discriminant analysis to more deeply characterize the microbiota alterations in LL-treated diabetic mice (Figure 7C). Genera with logarithmic LDA scores of >4.0 are plotted in Figure 7D, a circular cladogram based on the LEfSe results demonstrated differentially abundant taxa between three groups (Figure 7E). There were 15 taxa and 25 taxa with significant changes in the model and LL group. Overall, these results shows that *Parabacteroides*, *Parabacteroides_unclassified*, *Mucispirillum*, *Mucispirillum_schaedleri* could be the differential bacteria between model group and LL group.

Discussion

Previous research showed that the extract of *L. glutinosa* could significantly reduce the blood glucose. Intriguing by these findings, our group isolated and identified the chemical constituents of *L. glutinosa* and results indicated that lignans, alkaloids were the characteristic components(Wu et al., 2017) (Sun et al., 2019). Previously, we obtained the total alkaloid (CG) from *L. glutinosa* and investigated its anti-hyperglycemic effects in ob/ob mice (Zhang, et al. 2018). The results revealed that the alkaloid-rich extract of CG displayed potential anti-hyperglycemic and anti-hyperlipidemic effects. In this research, eight main alkaloids were identified in CG and Laurolitsine (LL) was the richest one among them. We speculate that LL is the active ingredient in modulating the anti-hyperglycemic and anti-hyperlipidemic effects of CG, and then we carried out experiment in vivo to confirm the glucose-and lipid-lowering effect, lastly we analyzed the overall and fine regulation of LL on intestinal flora in type 2 diabetic mice by 16sRNA sequencing. It was found that *Parabacteroides* was decreased significantly and *Mucispirillum* was increased evidently in db/db mice, which can be reversed after LL treatment. Thus, it can be seen that the changes of these key bacteria may be an important reason for the improvement of glucose and lipid metabolism in type 2 diabetic mice. Of course, it is necessary to further confirm the role of key bacteria in improving glucose and lipid metabolism by means of antibiotic treatment and fecal bacteria transplantation.

Although this study adds a new evidence for the relationship between the efficacy of traditional Chinese medicine and intestinal flora, this association needs to be further verified, such as whether new compounds are formed after the metabolism of LL through intestinal flora, the bioavailability, bioactivity and toxicity of the new compounds if formed need to be further studied. In addition, the effects of traditional Chinese medicine on specific bacteria can be divided into direct effects (promotion, inhibition and killing) (Xu, Chen et al. 2017, Feng, Ao et al. 2019) and indirect effects by affecting intestinal pH, secretion of antibacterial substances, intestinal mucosal barrier function and so on (Martel, Ojcius et al. 2017, Luo, Yue et al. 2020). Which of the above-mentioned types does the effect of LL on key bacteria belong to? These are what we need to explore later.

The intestinal flora plays a significant role in the metabolism of exogenous substances and drugs, a series of metabolites such as SCFAs (Chen, Liao et al. 2018, Cao, Yao et al. 2019), vitamins (Zhou, Tang et al. 2018) and secondary bile acids (Li, Wang et al. 2019) can be produced in this metabolic process. By

acting as signal molecules, energy and nutritional resources, these molecules can exert extensive effects on physiological processes such as intestinal and immune homeostasis (Nakkarach, Foo et al. 2021), energy metabolism (Wang, Li et al. 2020) and brain behavior (El Aidy, Dinan et al. 2014), and then improve disease. We can use multi-omics analysis to study the interaction between traditional Chinese medicine and intestinal flora. The joint analysis of genomics and metabolomics can avoid the influence of epigenetic modulation and post-translational modification of transcriptome and proteomics directly reflect the functional state of cells and are more likely to be associated with phenotypes. Therefore, metabonomics is an ideal tool to study the interaction between traditional Chinese medicine and intestinal flora. Through the comprehensive study, the complex interaction mechanism between host and intestinal flora can be systematically clarified, and the microorganisms and active compounds with important value in the treatment of TCM can be screened out.

Conclusions

In conclusion, our results indicate that Laurolitsine, an alkaloid obtained form *L. glutinosa*, have glucose- and lipid-lowering effects and improve diabetes-related symptoms in db/db mice. Modulation of the gut microbiota may play a role in the anti-diabetic effect of Laurolitsine.

Abbreviations

AST
aspartate aminotransferase
ALT
alanine aminotransferase
CG
total alkaloid of *Litsea glutinosa*
HDL-c
high-density lipoprotein cholesterol
HFD
high-fat diet
LL
Laurolitsine
LDA
linear discriminant analysis
LDL-c
low-density lipoprotein cholesterol
LEfSe
LDA Effect Size
PCoA
principal coordinate analysis

PCA
Principal Component Analysis
T2DM
Type 2 diabetes
TCM
Traditional Chinese Medicine
TC
total cholesterol
TG
total triglyceride

Declarations

Acknowledgments

Not applicable.

Authors' contributions

Rui-qi Wang: Methodology, Investigation, Formal analysis, Data curation, Writing - original draft, Writing - review & editing, Supervision. **Fang Zhang:** Investigation, Writing - original draft, Writing - review & editing. **Ya-nan Yang:** Software, Formal analysis. **Yong Zhang:** Investigation. **Yin-feng Tan:** Investigation. **Lin Dong:** Investigation. **Wei-ying Lu:** Investigation. **Ning Ma:** Investigation. **Chong-ming Wu:** Conceptualization, Project administration, Funding acquisition, Methodology, Investigation, Validation, Formal analysis, Data curation, Writing - original draft. **Xiao-po Zhang:** Funding acquisition, Methodology, Investigation, Validation, Writing - original draft.

Funding

The project was supported by Natural Science Foundation of Hainan Province (No.2019RC208), Natural Science Foundation of China (No.81760628), and Key Research and Development Program of Hainan Province (No.ZDYF2019157).

Availability of data and materials

The data are available from the corresponding author by appropriate request.

Ethics approval and consent to participate

Ethics approval and consent to participate animal experiment procedures were approved by the Medical Ethics Committee of Hainan Medical University (Permit Number: SYXK-2017-0013).

Consent for publication

Not applicable.

Competing interests

The authors declare that they have no conflicts of interest

Author details

[1]Key Laboratory of Tropical Translational Medicine of Ministry of Education, Hainan Key Laboratory for Research and Development of Tropical Herbs, School of Pharmacy, Hainan Medical University, Haikou, 57199, PR China.[2]Pharmacology and Toxicology Research Center, Institute of Medicinal Plant Development, Chinese Academy of Medical Sciences & Peking Union Medical College, Beijing, 100193, China.[3]Reproductive Medical Center, Hainan Women and Children's Medical Center, Haikou, China.

References

1. Bysani M, Agren R, Davegårdh C, Volkov P, Rönn T, Unneberg P, Bacos K, Ling C. ATAC-seq reveals alterations in open chromatin in pancreatic islets from subjects with type 2 diabetes. Sci Rep. 2019;9(1):7785.
2. Cao Y, Yao G, Sheng Y, Yang L, Wang Z, Yang Z, Zhuang P, Zhang Y. Jinqi Jiangtang tablet regulates gut microbiota and improve insulin sensitivity in type 2 diabetes mice. J Diabetes Res. 2019;1872134.
3. Caron A, Ahmed F, Peshdary V, Garneau L, Atlas E, Aguer C. Effects of PCB126 on adipose-to-muscle communication in an in vitro model. Environ Health Perspect. 2020;128(10):107002.
4. Chen M, Liao Z, Lu B, Wang M, Lin L, Zhang S, Li Y, Liu D, Liao Q, Xie Z. Huang-Lian-Jie-Du-Decoction ameliorates hyperglycemia and insulin resistant in association with gut microbiota modulation. Front Microbiol. 2018;9:2380.
5. Chen Y, Li Z, Hu S, Zhang J, Wu J, Shao N, Bo X, Ni M, Ying X. Gut metagenomes of type 2 diabetic patients have characteristic single-nucleotide polymorphism distribution in Bacteroides coprocola. Microbiome. 2017;5(1): 15.
6. Feng W, Ao H, Peng C, Yan D. Gut microbiota, a new frontier to understand traditional Chinese medicines. Pharmacol Res. 2019;142:176–191.
7. Gao K, Yang R, Zhang J, Wang Z, Jia C, Zhang F, Li S, Wang J, Murtaza G, Xie H, Zhao H, Wang W, Chen J. Effects of Qijian mixture on type 2 diabetes assessed by metabonomics, gut microbiota and network pharmacology. Pharmacol Res. 2018;130:93–109.
8. Ji Y, Wang C, Zhang Y, Zhang C, Cui D, Zhang X. Glutinosine A: a new morphinandienone alkaloid from Litsea glutinosa. Rec Nat Prod. 2019;13(4):363–366.
9. Ke XX, Walker A, Haange SB, Lagkouvardos I, Liu Y, Schmitt-Kopplin P, von Bergen M, Jehmlich N, He X, Clavel T, Cheung PCK. Synbiotic-driven improvement of metabolic disturbances is associated with changes in the gut microbiome in diet-induced obese mice. Mol Metab. 2019;22:96–109.

10. Li N, Wang B, Wu Y, Luo X, Chen Z, Sang C, Xiong T. Modification effects of SanWei GanJiang Powder on liver and intestinal damage through reversing bile acid homeostasis. Biomed Pharmacother. 2019;116:109044.
11. Li J, Yang S, Lei R, Gu W, Qin Y, Ma S, Chen K, Chang Y, Bai X, Xia S, Wu C, Xing G. Oral administration of rutile and anatase TiO(2) nanoparticles shifts mouse gut microbiota structure. Nanoscale. 2018;10(16):7736–7745.
12. Liu D, Zhang Y, Liu Y, Hou L, Li S, Tian H, Zhao T. Berberine modulates gut microbiota and reduces insulin resistance via the TLR4 signaling pathway. Exp Clin Endocrinol Diabetes. 2018;126(8):513–520.
13. Luo X, Yue B, Yu Z, Ren Y, Zhang J, Ren J, Wang Z, Dou W. Obacunone protects against ulcerative colitis in mice by modulating gut microbiota, attenuating TLR4/NF-κB signaling cascades, and improving disrupted epithelial barriers. Front Microbiol. 2020;11:497.
14. Martel J, Ojcius DM, Chang CJ, Lin CS, Lu CC, Ko YF, Tseng SF, Lai HC, Young JD. Anti-obesogenic and antidiabetic effects of plants and mushrooms. Nat Rev Endocrinol. 2017;13(3):149–160.
15. Molinaro A, Koh A, Wu H, Schoeler M, Faggi MI, Carreras A, Hallén A, Bäckhed F, Caesar R. Hepatic expression of lipopolysaccharide-binding protein (Lbp) is induced by the gut microbiota through Myd88 and impairs glucose tolerance in mice independent of obesity. Mol Metab. 2020;37:100997.
16. Nakkarach A, Foo HL, Song AA, Mutalib NEA, Nitisinprasert S, Withayagiat U. Anti-cancer and anti-inflammatory effects elicited by short chain fatty acids produced by Escherichia coli isolated from healthy human gut microbiota. Microb Cell Fact. 2021;20(1):36.
17. Jin Y, Wu Y, Li Y, Zhang C, Sun W, Dong L, Zhang X. Litsine A: A new aporphine alkaloid from the root barks of Litsea glutinosa. Rec Nat Prod. 2018;13:167–171.
18. Sun W, Jin Y, Zhang L, Tan Y, Zhang C, Dong L, Zhang X. Two new aminoethylstilbene isoquinoline alkaloids with glucose consumption increasing activity from the root barks of Litsea glutinosa. Phytochem Lett. 2019;34: 96–98.
19. Tan YF, Wang RQ, Wang WT, Wu Y, Ma N, Lu WY, Zhang Y, Zhang XP. Study on the pharmacokinetics, tissue distribution and excretion of laurolitsine from Litsea glutinosa in Sprague-Dawley rats. Pharm Biol. 2021;59: 884–892.
20. Wu Y, Jin Y, Dong L, Li Y, Zhang C, Gui M, Zhang X. New lignan glycosides from the root barks of Litsea glutinosa. Phytochem Lett. 2017;20:259–262.
21. Toda G, Soeda K, Okazaki Y, Kobayashi N, Masuda Y, Arakawa N, Suwanai H, Masamoto Y, Izumida Y, Kamei N, Sasako T, Suzuki R, Kubota T, Kubota N, Kurokawa M, Tobe K, Noda T, Honda K, Accili D, Yamauchi T, Kadowaki T, Ueki K. Insulin- and lipopolysaccharide-mediated signaling in adipose tissue macrophages regulates postprandial glycemia through Akt-mTOR activation. Mol Cell. 2020;79(1):43–53.
22. Wang J, Li W, Wang C, Wang L, He T, Hu H, Song J, Cui C, Qiao J, Qing L, Li L, Zang N, Wang K, Wu C, Qi L, Ma A, Zheng H, Hou X, Liu F, Chen L. Enterotype Bacteroides is associated with a high risk in patients with diabetes: a pilot study. J Diabetes Res. 2020;6047145.

23. Wu B, Huang XY, Li L, Fan XH, Li PC, Huang CQ, Xiao J, Gui R, Wang S. Attenuation of diabetic cardiomyopathy by relying on kirenol to suppress inflammation in a diabetic rat model. J Cell Mol Med. 2019;23(11):7651–7663.
24. Xu J, Chen HB, Li SL. Understanding the molecular mechanisms of the interplay between herbal medicines and gut microbiota. Med Res Rev. 2017;37(5):1140–1185.
25. Yang MH, Chen M, Mo HH, Tsai WC, Chang YC, Chang CC, Chen KC, Wu HY, Yuan CH, Lee CH, Chen YA, Tyan YC. Utilizing Experimental Mouse Model to Identify Effectors of Hepatocellular Carcinoma Induced by HBx Antigen. Cancers (Basel). 2020;12(2):409.
26. Zhang B, Yue R, Chen Y, Yang M, Huang X, Shui J, Peng Y, Chin J. Gut microbiota, a potential new target for Chinese Herbal Medicines in treating diabetes mellitus. Evid Based Complement Alternat Med. 2019;2634898.
27. Zhang XP, Jin Y, Wu YN, Jin DJ, Zheng QX, Li YB. Anti-hyperglycemic and anti-hyperlipidemia effects of the alkaloid-rich extract from barks of Litsea glutinosa in ob/ob mice. Sci Rep. 2018;8:12646.
28. Zhou J, Tang L, Shen CL, Wang JS. Green tea polyphenols modify gut-microbiota dependent metabolisms of energy, bile constituents and micronutrients in female Sprague-Dawley rats. J Nutr Biochem 2018;61:68–81.

Figures

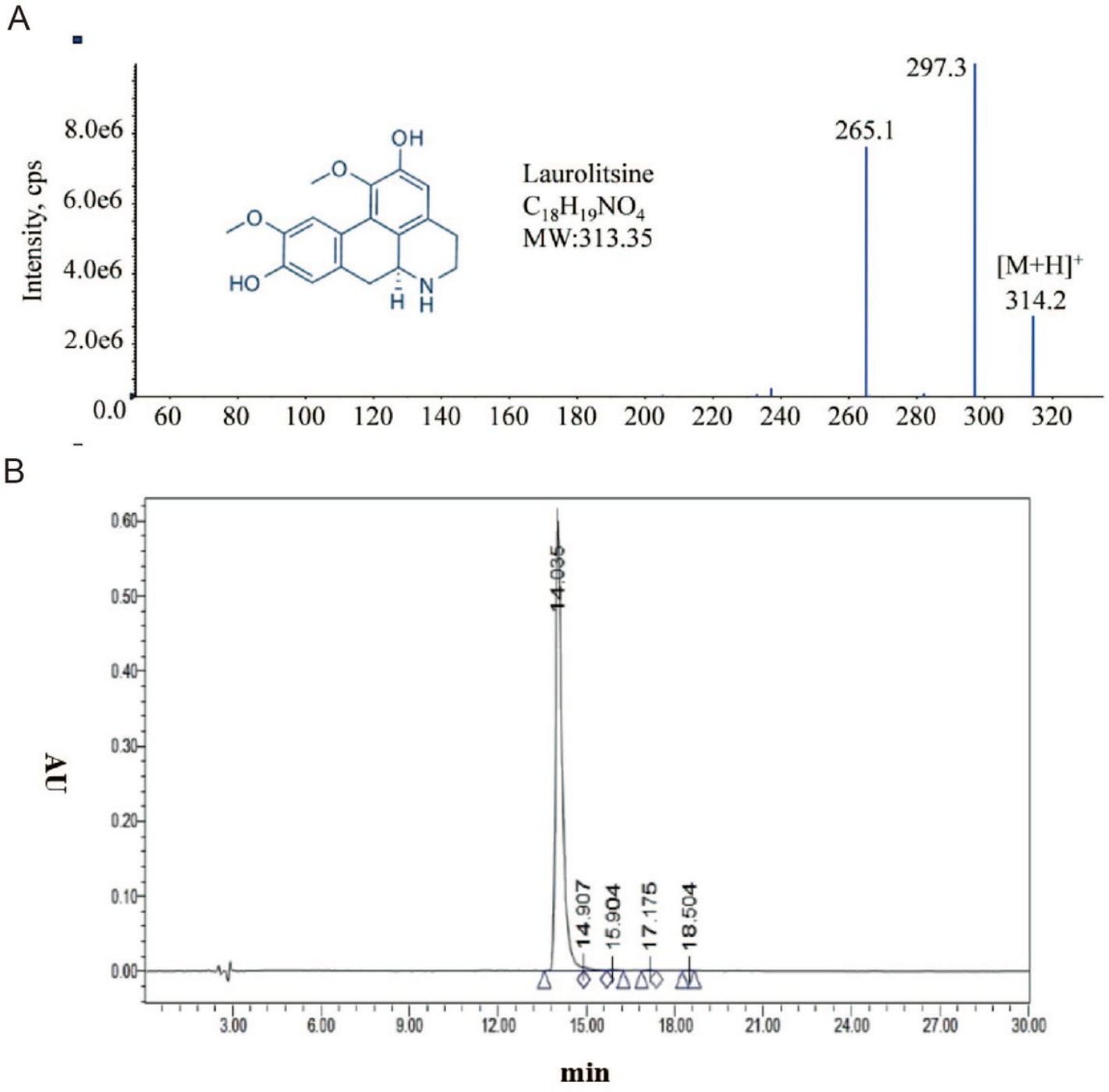

Figure 1

The structural identification of LL. (A) MS spectrum of LL. (B) The HPLC spectrum of LL (Retention time = 14.035 min).

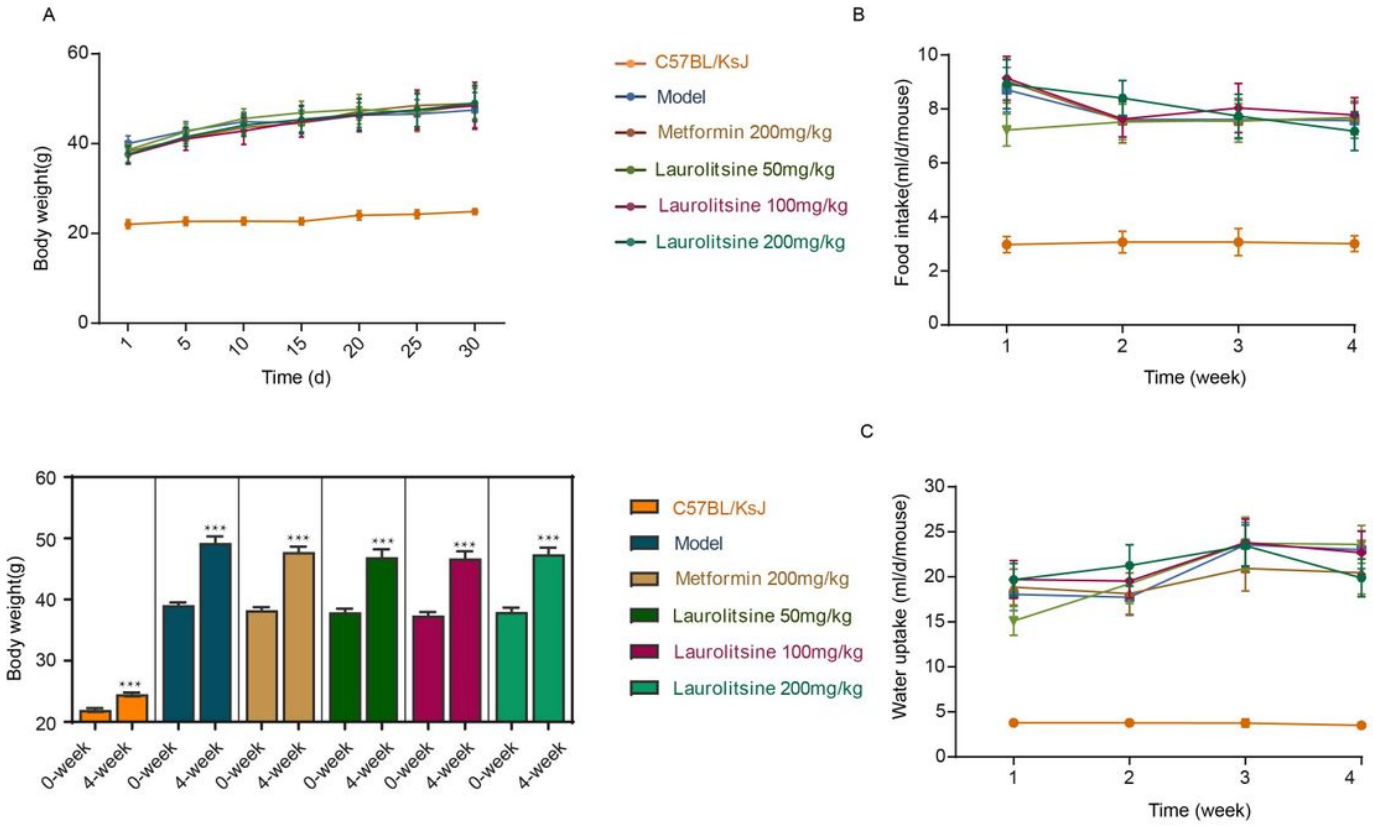

Figure 2

The effects of LL on body weight, food intake and water uptake in db/db mice. The mice were divided into 6 groups, including C57BL/KsJ group (n = 10), model group (n = 10), LL 50 mg·Kg-1 group (n = 10), LL 100 mg·Kg-1 group (n = 10), LL 200 mg·Kg-1 group (n = 10), and metformin 200 mg·Kg-1 group (n = 10). (A) Body weight of mice in each group from 1 to 30 days and comparison of weight changes of mice in each group at 0 and 4 weeks. (B) Food intake (g/d/mouse) of mice in each group from 1 to 4 weeks. (C) Water uptake (ml/d/mouse) of mice in each group from 1 to 4 weeks.

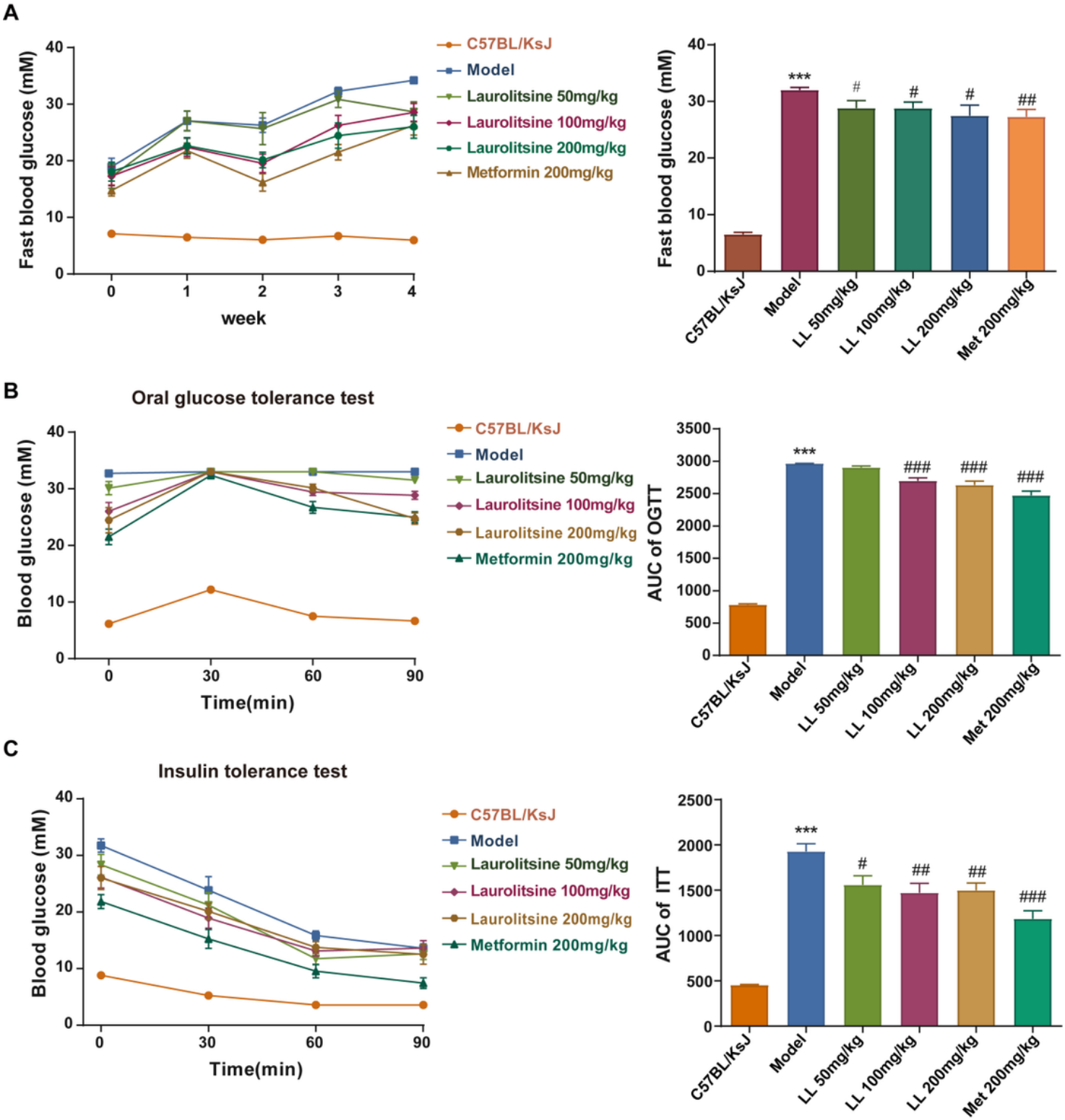

Figure 3

The effects of LL on glucose metabolism. (A) Fast food glucose (mM) in each group from 0 to 4 weeks (left) and comparison of Fasting Glucose (mM) in each group at 4 weeks (right). (B) Changes of blood glucose level in oral glucose tolerance test (OGTT) at four different time points (0, 30, 60, 90 minutes) (left) and area under curve (AUC) for the OGTT in each group (right). (C) Changes of blood glucose level in insulin tolerance test (ITT) at four different time points (0, 30, 60, 90 minutes) (left) and area under

curve (AUC) for the ITT in each group (right). Compared with control group, ***P0.001; compared with model group, #P<0.05, ##P0.01, ###P0.001.

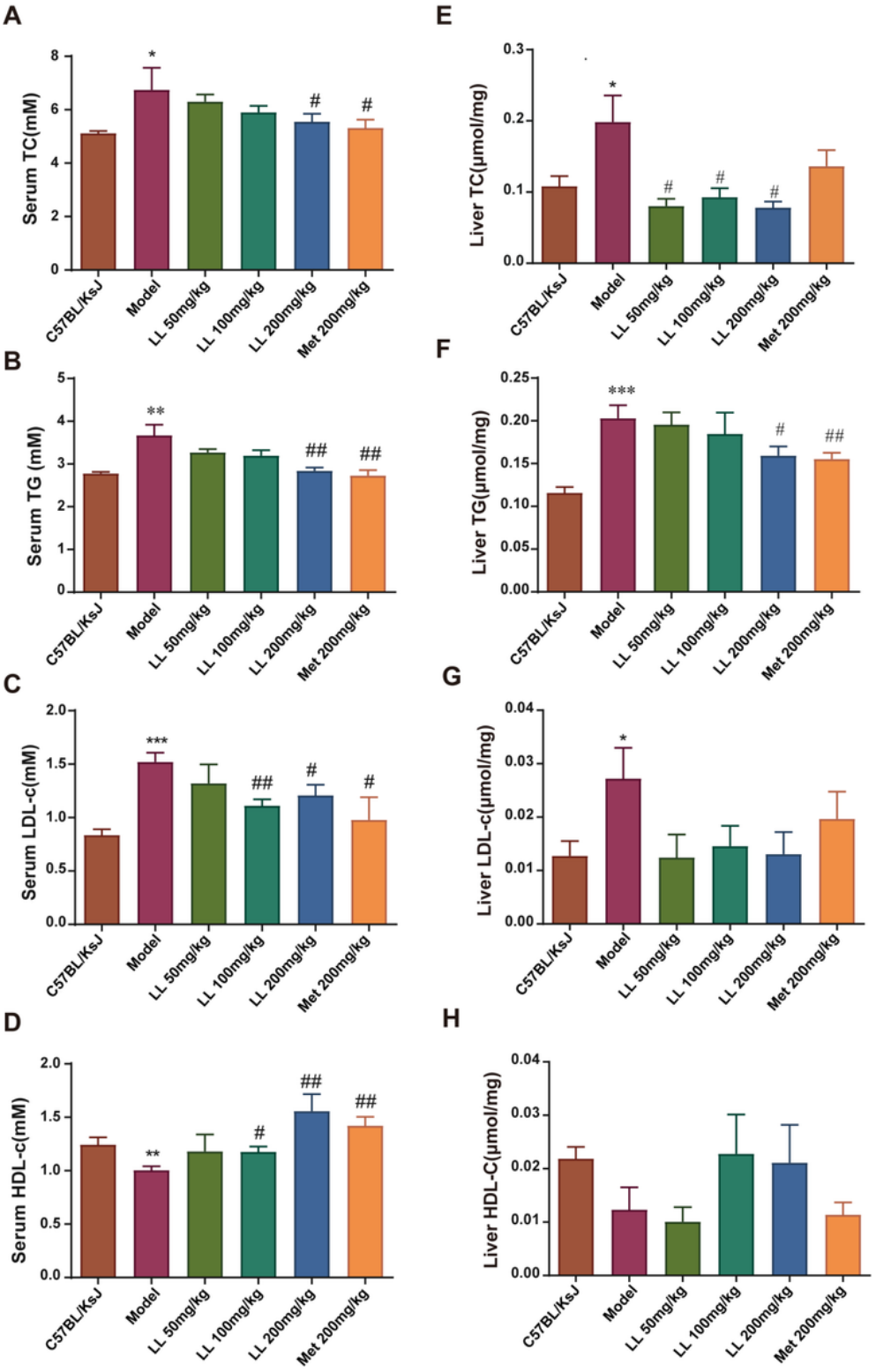

Figure 4

Effects of LL on (A) serum total cholesterol (TC), (B) serum triglyceride (TG), (C) serum low-density lipoprotein cholesterol (LDL-c), (D) serum high-density lipoprotein cholesterol (HDL-c), (E) liver TC, (F) liver

TG, (G) liver LDL-c and (H) liver HDL-c in mice among each group. Compared with control group,*P 0.05**P 0.01***P 0.001; compared with model group, #P<0.05, ##P0.01.

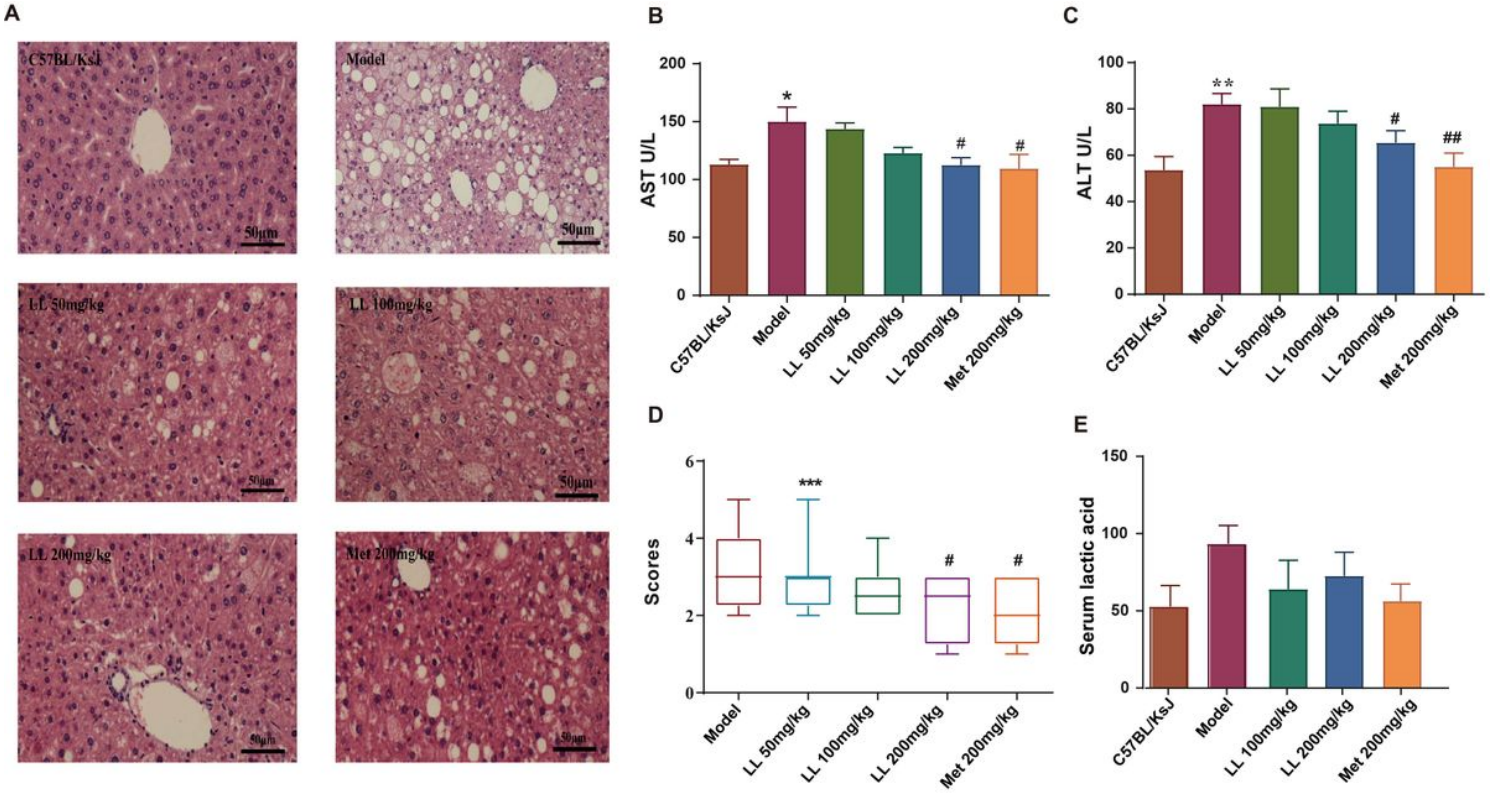

Figure 5

The effects of LL on liver function. (A) Representative hematoxylin and eosin (H&E) staining images of the liver, Effect of LL on (B) AST level and (C) ALT level among each group. (D) Pathological scores in model, LL and metformin group. (E) Serum level of lactic acid in each group. Compared with control group,*P 0.05**P 0.01***P 0.001; compared with model group, #P < 0.05, ##P 0.01.

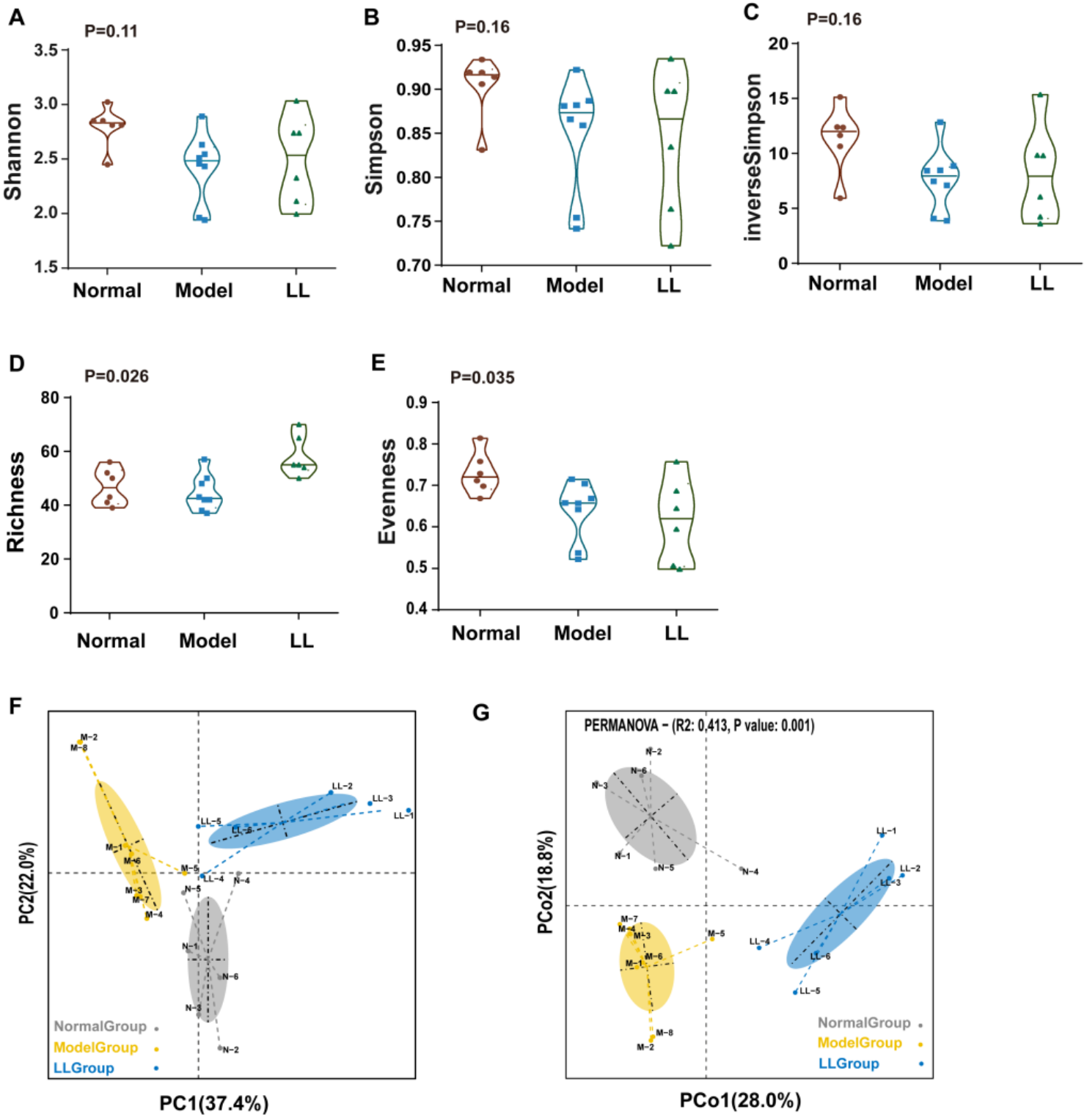

Figure 6

The effect of LL on structure of the gut microbiota in each group mice. The alpha diversity of the gut microbiota in normal group, model group and LL group were measured by the (A) Shannon index, (B) Simpson index, (C) inverse Simpson index, (D) Richness index and (E) Evenness index. The beta diversity of the gut microbiota in normal group, model group and LL group were measured by (F) Principal component analysis (PCA) and principal coordinate analysis (PCoA).

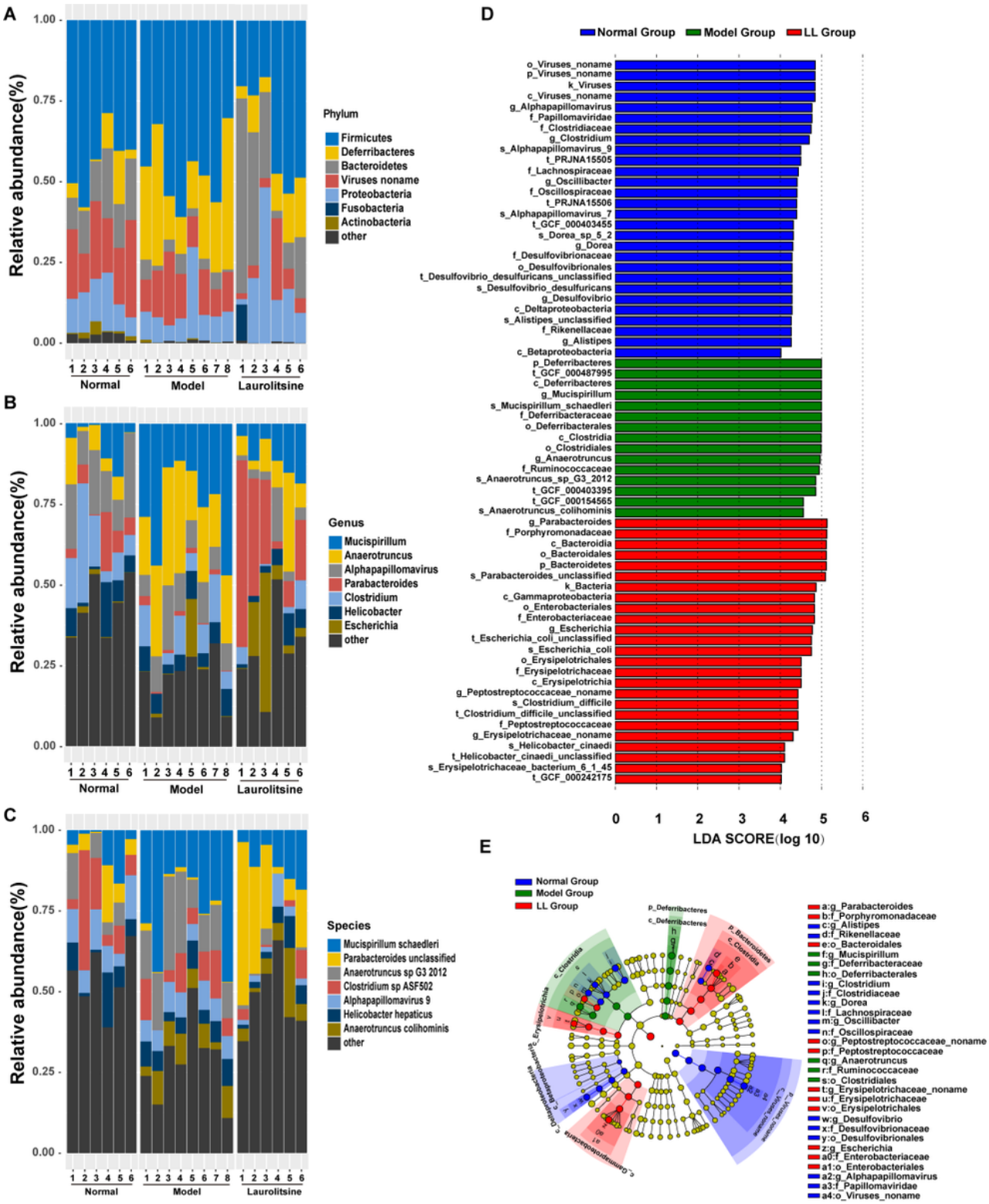

Figure 7

The effect of LL on composition of the gut microbiota in each group. The relative abundances of predominant different bacteria among normal group, model group and LL group were shown at the (A) phylum-level, (B) genus-level, and (C) species-level. Stacked bar graphs illustrate the abundances of phyla, genera and species. (D) Linear discriminant analysis effect size (LEfSe) and LDA analysis (LDA Score >4.0, P < 0.05) based on OTUs characterize the microbiomes in normal group, model group and LL

group.(E) LEfSe analysis identifying the significantly abundant taxon among normal group, model group and LL group.

Supplementary Files

This is a list of supplementary files associated with this preprint. Click to download.

- GraphicAbstract.jpeg